Astrophys Space Sci (2008) 314: 193–197
DOI 10.1007/s10509-008-9754-2

ORIGINAL ARTICLE

Synchrotron self-Compton models of high brightness temperature radio sources

Olivia Tsang · J.G. Kirk

Received: 7 January 2008 / Accepted: 28 January 2008 / Published online: 22 February 2008

Abstract We re-examine the maximum brightness temperature that a synchrotron source can sustain by adapting standard synchrotron theory to an electron distribution that exhibits a deficit at low energy. The absence of low energy electrons reduces the absorption of synchrotron photons, allowing the source to reach a higher brightness temperature without the onset of catastrophic cooling. We find that a temperature of $\sim 10^{14}$ K is possible at GHz frequencies. In addition, a high degree of intrinsic circular polarisation is produced. We compute the stationary, synchrotron and self-Compton spectrum arising from the continuous injection of such a distribution (modelled as a double power-law) balanced by radiative losses and escape, and compare it with the simultaneously observed multi-wavelength spectrum of the BL Lac object S5 0716+714. This framework may provide an explanation of other high brightness-temperature sources without the need for mechanisms such as coherent emission or proton synchrotron radiation.

Keywords Galaxies · Active galaxies · High redshift galaxies · Jets

1 Introduction

In the standard theory for the synchrotron radiation of a power-law distribution of electrons $\mathrm{d}(\ln n_\mathrm{e})/\mathrm{d}(\ln\gamma) = -p$ (with $p \geq 1$), the spectrum peaks at roughly the frequency $\nu = \nu_\mathrm{abs}$ where the optical depth to synchrotron self-absorption is unity. At higher frequencies, the specific intensity falls off as $I_\nu \propto \nu^{-(p-1)/2}$; at lower frequencies as $I_\nu \propto \nu^{5/2}$. The brightness temperature $T_\mathrm{B} = c^2 I_\nu/(2\nu^2 k_\mathrm{B})$ also peaks at this point. For this scenario, Kellermann and Pauliny-Toth (1969) found that the luminosity of inverse Compton scattered synchrotron photons increases rapidly with the peak value T_max of brightness temperature, specifically as T_max^5, when T_max is above a threshold temperature T_thresh. The exact value of T_thresh depends on the source parameters, (see, for example, Readhead 1994) but for a synchrotron spectrum peaking at GHz frequencies, $T_\mathrm{thresh} \approx 10^{12}$ K.

The intra-day variability observed in some extra-galactic radio sources, whether due to intrinsic variations or to interstellar scintillation, suggests that these sources have brightness temperature well over 10^{12} K, (Wagner and Witzel 1995) sometimes by a few orders of magnitude. These observations cannot be explained by the synchrotron theory described above, without invoking excessive Doppler boosting. It has been suggested that such high brightness temperatures indicate a different emission mechanism, such as coherent emission (e.g., Begelman et al. 2005) or proton synchrotron radiation (Kardashev 2000).

Here we present a reassessment of the problem using a distribution that has a deficit of low energy, but still relativistic, electrons whose Lorentz factor is less than a certain value: $\gamma < \gamma_\mathrm{p}$. As is well-known (e.g., Longair 1992), the brightness temperature of a synchrotron source at a frequency ν is limited by the energy $\gamma m_\mathrm{e} c^2$ of those electrons that dominate the opacity at that frequency: $T_\mathrm{B} \lesssim \gamma m_\mathrm{e} c^2/k_\mathrm{B}$, the maximum value being reached when the source becomes optically thick. Thus, a distribution with a deficit of low energy electrons can permit a higher brightness temperature at $\nu = \nu_\mathrm{abs}$ than can be achieved with the standard power-law distribution. This is the case, for example, for a relativistic Maxwellian distribution with temperature $T \approx \gamma_\mathrm{p} m_\mathrm{e} c^2/k_\mathrm{B}$. Higher energy electrons with $\gamma > \gamma_\mathrm{p}$

O. Tsang · J.G. Kirk (✉)
Max-Planck-Institut für Kernphysik, Heidelberg, Germany
e-mail: kirk@mpi-hd.mpg.de

can be added to this distribution without affecting the value of $T_{\max} \approx \gamma_{\rm p} m_{\rm e} c^2/k_{\rm B}$, provided that their number falls off to higher energy more rapidly than a power-law with $p = 1/3$.

For low frequency radiation, such a distribution can be well-approximated as monoenergetic on a linear frequency scale. We therefore start off by reviewing, in Sect. 2, the results concerning maximum brightness temperature and circular polarisation (Kirk and Tsang 2006; Tsang and Kirk 2007) obtained with this approximation. Since high frequency radiation is sensitive to the electron distribution at $\gamma > \gamma_{\rm p}$, we then, in Sect. 3, relax the monoenergetic approximation in favour of a double power-law electron injection function $Q(\gamma)$. Specifically, we choose $\mathrm{d}(\ln Q)/\mathrm{d}(\ln \gamma) = 2$ for $\gamma < \gamma_{\rm p}$, which corresponds approximately to the relativistic Maxwellian, (and, therefore, permits relatively high brightness temperatures at low frequency) and combine it with $\mathrm{d}(\ln Q)/\mathrm{d}(\ln \gamma) \approx -2.3$ for $\gamma_{\rm p} < \gamma < \gamma_{\max}$, as suggested by theories of particle acceleration at relativistic shocks (Kirk et al. 2000; Achterberg et al. 2001). This allows us to compute the entire synchrotron self-Compton spectrum. For comparison with multi-wavelength observations, the best published set of simultaneously taken data appears to be that for the source 5 0716+714 (Ostorero et al. 2006). In Sect. 4 we compare our model to these measurements.

2 Brightness temperature and circular polarisation

We consider a homogeneous source region characterised by a single spatial scale R, that contains monoenergetic electrons of Lorentz factor γ and number density $N_{\rm e}$ immersed in a homogeneous magnetic field B. The synchrotron emissivity and absorption coefficients are given in many texts (e.g., Rybicki and Lightman 1979, Chapter 6), and are summarised in our notation by Tsang and Kirk (2007). The low frequency, optically thin spectrum is quite flat ("hard" in the language of high-energy astrophysics): $-1/3 \le \alpha \lesssim 0$ for $I_\nu \propto \nu^{-\alpha}$. This is a promising property for the interpretation of flat spectrum radio sources. However, it is not present in all cases. In very compact sources, where the synchrotron spectrum changes from optically thick to optically thin at a frequency greater than the characteristic frequency $\nu_{\rm s} = 3eB\gamma^2 \sin\theta/(4\pi mc)$, ($\theta$ is the angle between the line of sight and the magnetic field) the synchrotron emission is quite sharply peaked at $\nu_{\rm abs}$, rising as $I_\nu \propto \nu$ between $\nu_{\rm s}$ and $\nu_{\rm abs}$, the frequency at which the plasma becomes optically-thick, and cutting off sharply towards higher frequencies (Tsang and Kirk 2007).

Five input parameters are required to specify the source model: the Doppler boosting factor $\mathcal{D}$, size R, electron Lorentz factor γ, magnetic field strength B, and electron density $N_{\rm e}$. The first is constrained by surveys of superluminal motion (Cohen et al. 2003) to be at most of the order of 10. For scintillating sources, an upper limit on the size can be found, given an estimate of the screen distance. For intrinsically varying sources, the corresponding limit constrains the combination $R/\mathcal{D}^2$. However, the quantities γ, B, and $N_{\rm e}$ are less accessible. Because of this, it is convenient to express them in terms of three different parameters:

1. the optical depth to synchrotron self-absorption, $\tau_{\rm s}$, at the observing frequency ν:

$$\tau_{\rm s}(\nu) = \frac{\sqrt{3}\tau_{\rm T} m_{\rm e} c^3 K_{5/3}(x)}{8\pi e^2 \nu_{\rm s} \gamma^3} \tag{1}$$

   where $\tau_{\rm T} = N_{\rm e}\sigma_{\rm T} R$ is the Thomson optical depth, $K_{5/3}(x)$ is a modified Bessel function,

$$x = \nu(1+z)/(\mathcal{D}\nu_{\rm s}) \tag{2}$$

   and z is the redshift of the host galaxy,
2. the parameter

$$\xi = 4\gamma^2 \tau_{\rm T}/3 \tag{3}$$

   that controls the ratio of the inverse Compton to the synchrotron luminosity (see Kirk and Tsang 2006), and
3. the characteristic synchrotron frequency $\nu_{\rm s}$, above which the spectrum of a monoenergetic electron distribution cuts off exponentially. This is roughly the frequency up to which the optically thin spectrum remains flat (hard), and is written below as $\nu_{\max,14} = \nu_{\rm s}/(10^{14}\ \mathrm{Hz})$.

At low frequencies, such that $\nu/\nu_{\rm s} \ll 1$, one finds for the brightness temperature observed at Earth:

$$T_{\rm B} = 1.2 \times 10^{14} \left[\frac{\mathcal{D}_{10}^6 \xi}{(1+z)^6}\right]^{1/5} \left(\frac{1-\mathrm{e}^{-\tau_{\rm s}}}{\tau_{\rm s}^{1/5}}\right) \nu_{\max,14}^{2/15} \nu_{\rm GHz}^{-1/3}\ \mathrm{K} \tag{4}$$

where $\mathcal{D}_{10} = \mathcal{D}/10$ and $\nu_{\rm GHz}$ is the observing frequency in GHz. Thus, brightness temperatures of up to roughly 10^{13} K at GHz frequencies can be achieved with $\xi \lesssim 1$ (i.e., with modest inverse Compton luminosity) without Doppler boosting, whereas, with reasonable boosting factors, brightness temperatures of roughly $T_{\rm B} \sim 10^{14}$ K are possible.

As well as very high brightness temperature, several intra-day variable radio sources display a relatively high degree of circular polarisation $r_{\rm c} \approx 1\%$ (Macquart 2003). In conventional models, where the opacity is dominated by electrons whose characteristic synchrotron frequency is close to the observing frequency, the intrinsic circular polarisation is $r_{\rm c} \sim m_{\rm e} c^2/(k_{\rm B} T_{\rm B})$, far too small to explain the observations. However, if the electron distribution is deficient at low energies, the observing frequency is typically much smaller than the characteristic synchrotron frequency: $\nu \ll \nu_{\rm s}$. In this case, the intrinsic circular polarisation is

much stronger:

$$r_{\rm c} = 1.9 \times 10^{-2} \left(\frac{\tau_{\rm s}}{\mathcal{D}_{10} \xi} \right)^{1/5} \nu_{\rm max,14}^{1/5} \cot\theta \tag{5}$$

This expression is relatively insensitive to all the source parameters except the direction of the magnetic field, suggesting that the observed polarisation may indeed be of intrinsic origin.

3 Broken power-law electron injection

In order to model the high energy emission produced by inverse Compton scattering of the synchrotron photons produced in the source (SSC model), the distribution of high energy electrons must be modelled. This can be done without significantly affecting the conclusions of the previous section by postulating a double power-law injection function. In general, this takes the form

$$Q(\gamma) = Q_0 \begin{cases} (\gamma/\gamma_{\rm p})^{-p_1}, & \gamma_{\rm min} \le \gamma < \gamma_{\rm p} \\ (\gamma/\gamma_{\rm p})^{-p_2}, & \gamma_{\rm p} \le \gamma < \gamma_{\rm max} \end{cases} \tag{6}$$

However, when modelling intra-day variables, it is sufficient to choose $p_1 = -2$, mimicking a relativistic Maxwellian at low energies, in which case $\gamma_{\rm min}$ is irrelevant and can safely be set to unity.

The electron distribution $n_{\rm e} = {\rm d}N_{\rm e}/{\rm d}\gamma$ that results from this injection function is found as the stationary solution of the kinetic equation:

$$\frac{\partial n_{\rm e}}{\partial t} + \frac{\partial}{\partial \gamma}(n_{\rm e}\dot{\gamma}) + \frac{n_{\rm e}}{t_{\rm esc}} = Q(\gamma) \tag{7}$$

where $\dot{\gamma}$ is the radiative cooling rate of the electrons and $t_{\rm esc}$ is a timescale that takes account of the energy independent loss of particles from the source region, for example by advection across its boundaries. Because the synchrotron component dominates the radiative output in the models we present, cooling by inverse Compton scattering can be neglected, so that

$$\dot{\gamma} = -\frac{4\sigma_{\rm T} U_{\rm B} \gamma^2}{3 m_{\rm e} c} \tag{8}$$

with the energy density in the magnetic field given by $U_{\rm B} = B^2/(8\pi)$. Defining the Lorentz factor $\gamma_{\rm c}$ at which the radiative cooling rate equals the particle loss rate:

$$\gamma_{\rm c} = \frac{3 m_{\rm e} c}{4\sigma_{\rm T} U_{\rm B} t_{\rm esc}} \tag{9}$$

so that $\dot{\gamma} t_{\rm esc}/\gamma = \gamma/\gamma_{\rm c}$, one can formally write the stationary solution to Eq. (7) as

$$n_{\rm e}(\gamma) = \frac{t_{\rm esc}\gamma_{\rm c} {\rm e}^{-\gamma_{\rm c}/\gamma}}{\gamma^2} \left[\int_{\gamma}^{\gamma_{\rm max}} {\rm d}\gamma' Q(\gamma') {\rm e}^{\gamma_{\rm c}/\gamma'} \right] \tag{10}$$

given that $n_{\rm e}(\gamma)$ vanishes for $\gamma > \gamma_{\rm max}$. However, more insight is gained, and, at this level of modelling, no significant features are lost, by adopting the following procedure: construct the approximate solutions that result from dropping the particle loss term for $\gamma \gg \gamma_{\rm c}$ and dropping the radiative loss term for $\gamma \ll \gamma_{\rm c}$, and extrapolate these to the point where they intersect, which lies close to $\gamma = \gamma_{\rm c}$. Denoting this point (which depends weakly on $p_{1,2}$) by $\gamma_{\rm b}$, the resulting distribution is:

$$n_{\rm e} = \begin{cases} t_{\rm esc} Q(\gamma), & \gamma_{\rm min} \le \gamma < \gamma_{\rm b} \\ \frac{t_{\rm esc}\gamma_{\rm c}}{\gamma^2} \int_{\gamma}^{\gamma_{\rm max}} Q(\gamma'){\rm d}\gamma', & \gamma_{\rm b} \le \gamma < \gamma_{\rm max} \end{cases} \tag{11}$$

If $\gamma_{\rm c}$ (strictly speaking, $\gamma_{\rm b}$) lies above the peak of the injection function, $\gamma_{\rm p}$, the synchrotron spectrum has a break at the corresponding frequency from $\alpha = (p_2 - 1)/2$ at lower frequencies to $p_2/2$ at higher frequencies. On the other hand, if $\gamma_{\rm c}$ lies below the injection peak, the synchrotron spectrum between the frequencies corresponding to $\gamma_{\rm b}$ and $\gamma_{\rm p}$ has $\alpha = 0.5$, and breaks to $\alpha = -1/3$ (in the optically thin case) to lower frequencies.

4 Synchrotron self-Compton emission

The specific intensity I_ν^0 of synchrotron radiation is obtained from the radiative transport equation by standard means:

$$\begin{aligned} I_\nu^0 &= \frac{J_\nu}{4\pi\alpha_\nu}(1 - {\rm e}^{-\alpha_\nu \cdot R}) \\ &= -2m\nu^2 \frac{(1 - {\rm e}^{-\alpha_\nu \cdot R}) \int_{\gamma_{\rm min}}^{\gamma_{\rm max}} F(x) n_{\rm e}(\gamma) {\rm d}\gamma}{\int_{\gamma_{\rm min}}^{\gamma_{\rm max}} \gamma^2 F(x) \frac{\rm d}{{\rm d}\gamma}(\frac{n_{\rm e}(\gamma)}{\gamma^2}) {\rm d}\gamma} \end{aligned} \tag{12}$$

where J_ν is the specific emissivity and α_ν is the absorption coefficient. From this, the successive generations of self-Compton emission, labelled by i, follow from

$$I_\nu^{(i)} = \frac{4\pi}{3}\sigma_{\rm T}\nu R \int_{\gamma_{\rm min}}^{\gamma_{\rm max}} \frac{{\rm d}\gamma}{\gamma^2} n_{\rm e}(\gamma) \int_0^\infty \frac{{\rm d}\nu'}{\nu'^2} I_{\nu'}^{(i-1)} f(z) \tag{13}$$

(Georganopoulos et al. 2001) where $f(z)$, which fully accounts for Klein-Nishina effects, is defined by

$$\begin{aligned} f(z) &= \Big[2z\ln z + z + 1 - 2z^2 \\ &\quad + \frac{(4\epsilon_0\gamma z)^2(1-z)}{2(1+4\epsilon_0\gamma z)} \Big] P(1/4\gamma^2, 1, z) \\ z &= \frac{\epsilon}{4\epsilon_0\gamma^2(1-\epsilon/\gamma)} \\ \epsilon_0 &= h\nu'/(m_{\rm e}c^2) \\ \epsilon &= h\nu/(m_{\rm e}c^2) \\ P(1/4\gamma^2, 1, z) &= \begin{cases} 1 & \text{for } 1/4\gamma^2 \le z \le 1 \\ 0 & \text{otherwise} \end{cases} \end{aligned} \tag{14}$$

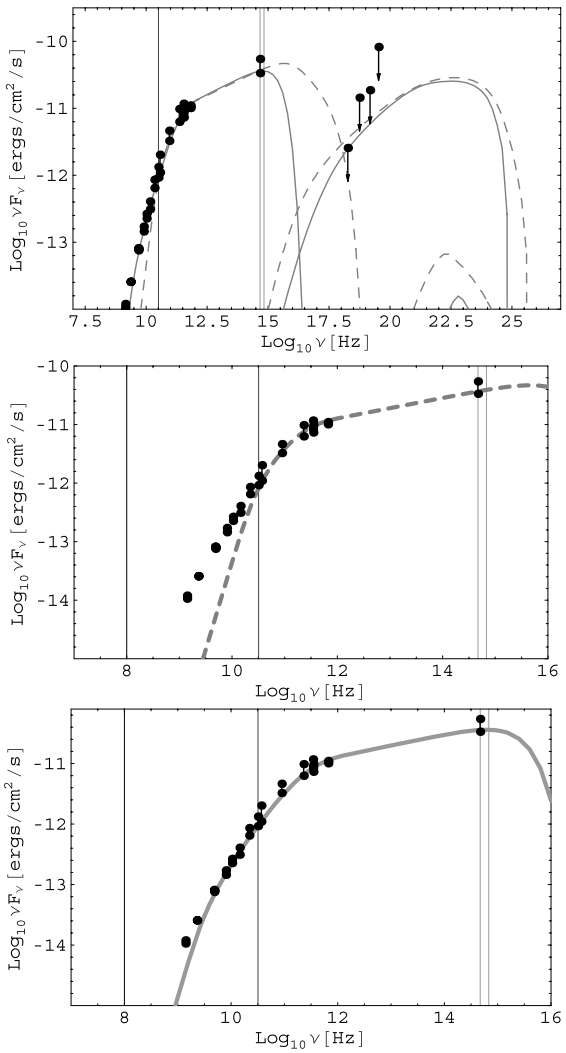

Fig. 1 The spectral energy distribution of S5 0716+714 from the multi-wavelength, simultaneous data set of Ostorero et al. (2006). The short-timescale variability at a given frequency is indicated by vertical bars connecting two points. INTEGRAL upper limits are also shown. The models discussed in the text are shown as *solid* (high $\mathcal{D}$) and *dashed* (low $\mathcal{D}$) *lines*. The *upper panel* shows the synchrotron emission and the first two generations of inverse Compton scattered photons. The *lower panels* show the synchrotron emission. Vertical lines indicate the optical band, 32 GHz and 100 MHz

The integrations in (12) and (13) are evaluated numerically over fixed grids in Lorentz factor and frequency.

As an example, we compare, in Fig. 1, two model fits to the extensive simultaneous multi-frequency coverage of the BL Lac object S5 0716+714 presented by Ostorero et al. (2006). This source was seen to vary on a timescale of 4.1 days at 32 GHz and 37 GHz, implying a very high brightness temperature. However, although the source spectrum continues to lower frequencies without a break, it is not clear whether the rapid variability persists at these frequencies. We therefore present one model (shown as solid lines) in which the lower frequency emission is produced within the rapidly variable source, and another in which we relax this constraint, and assume the radiation at $\nu < 32$ GHz is emitted from a much larger region. In this case, our source spectrum (dashed lines) is strongly self-absorbed below 32 GHz and passes well below the observed flux.

To obtain the fit shown by the solid line, we took a power-law index $p_2 = 2.6$, determined by the spectral index between 664 GHz and the optical band. The spectral index in the 5–500 GHz range is close $\alpha = -1/3$. This follows naturally from the model if p_1 is sufficiently small (we chose $p_1 = -2$, corresponding to a relativistic Maxwellian). The values of $\gamma_p = 696$ and $\gamma_c = 6 \times 10^6$ are chosen to place the contribution of electrons with $\gamma = \gamma_p$ close to 500 GHz, and the values of $\xi = 10^{-1.14}$ and $\mathcal{D} = 65$ are determined by the flux levels at 500 GHz and at 10^{19} Hz.

Note that this rather large value of the Doppler boosting factor is a lower limit, since the measurements at 10^{19} Hz are upper limits from INTEGRAL. Analysis of the historical data of VLBI images by Bach et al. (2005) reveals proper motion at roughly 20–30c, implying that the Doppler factor should also be $\sim$ 20–30. Consequently, either the jet components were moving much faster during the observations of Ostorero et al. (2006), or the radio emission below 32 GHz stems from a larger source region. Following up on the latter possibility, our second fit was obtained with $\mathcal{D} = 30$. Combined with $\gamma_p = 244$, $\gamma_c = 7.9 \times 10^4$ and $\xi = 10^{-1.35}$, this model fits all data points quite well for $\nu > 32$ GHz, where it has a brightness temperature in the frame of the observer of $T_B = 1.1 \times 10^{13}$ K. This low $\mathcal{D}$ fit would imply that the variability of the source is less rapid at low frequencies—something that can be checked by observation.

5 Summary

We have shown that high brightness temperature of the order of 10^{14} K is possible in standard synchrotron theory if the electron distribution is deficient at low energies. Such an electron distribution gives rise to flat, optically thin spectra, and a relatively high degree of intrinsic circular polarisation, of the order of 1%.

This model provides a good fit to multi-wavelength observations of the variable blazar S5 0716+714. It predicts emission from the first generation of inverse Compton scattered photons up to energies of the order of 10 GeV, at a flux level that should be detectable by GLAST. This approach provides a simple framework for explaining the observations of other high brightness temperature compact sources without the need for more exotic mechanisms such as coherent emission (Begelman et al. 2005) and proton synchrotron radiation (Kardashev 2000).

References

Achterberg, A., Gallant, Y.A., Kirk, J.G., Guthmann, A.W.: Particle acceleration by ultrarelativistic shocks: theory and simulations. Mon. Not. R. Astron. Soc. **328**, 393–408 (2001). doi:10.1046/j.1365-8711.2001.04851.x

Bach, U., Krichbaum, T.P., Ros, E., Britzen, S., Tian, W.W., Kraus, A., Witzel, A., Zensus, J.A.: Kinematic study of the blazar *S5 0716+714*. Astron. Astrophys. **433**, 815–825 (2005). doi:10.1051/0004-6361:20040388

Begelman, M.C., Ergun, R.E., Rees, M.J.: Cyclotron maser emission from blazar jets? Astrophys. J. **625**, 51–59 (2005). doi:10.1086/429550

Cohen, M.H., Russo, M.A., Homan, D.C., Kellermann, K.I., Lister, M.L., Vermeulen, R.C., Ros, E., Zensus, J.A.: Variability and velocity of superluminal sources. In: ASP Conf. Ser. 300: Radio Astronomy at the Fringe, p. 177 (2003)

Georganopoulos, M., Kirk, J.G., Mastichiadis, A.: The beaming pattern and spectrum of radiation from inverse Compton scattering in blazars. Astrophys. J. **561**, 111–117 (2001). doi:10.1086/323225

Kardashev, N.S.: Radio synchrotron emission by protons and electrons in pulsars and the nuclei of quasars. Astron. Rep. **44**, 719–724 (2000). doi:10.1134/1.1320497

Kellermann, K.I., Pauliny-Toth, I.I.K.: The spectra of opaque radio sources. Astrophys. J. **155**, L71 (1969)

Kirk, J.G., Tsang, O.: High brightness temperatures and circular polarisation in extra-galactic radio sources. Astron. Astrophys. **447**, L13–L16 (2006). doi:10.1051/0004-6361:200500231

Kirk, J.G., Guthmann, A.W., Gallant, Y.A., Achterberg, A.: Particle acceleration at ultrarelativistic shocks: an eigenfunction method. Astrophys. J. **542**, 235–242 (2000). doi:10.1086/309533

Longair, M.S.: High Energy Astrophysics, vol. 1, 2: Particles, Photons and Their Detection, 2nd edn. Cambridge University Press, Cambridge (1992)

Macquart, J.P.: Circular polarization in relativistic jets. New Astron. Rev. **47**, 609–612 (2003). doi:10.1016/S1387-6473(03)00104-0

Ostorero, L., Wagner, S.J., Gracia, E.A.J.: Testing the inverse-Compton catastrophe scenario in the intra-day variable blazar *S5 0716+71*. Astron. Astrophys. **451**, 797–807 (2006). doi:10.1051/0004-6361:20054075

Readhead, A.C.S.: Equipartition brightness temperature and the inverse Compton catastrophe. Astrophys. J. **426**, 51–59 (1994). doi:10.1086/174038

Rybicki, G.B., Lightman, A.P.: Radiative Processes in Astrophysics. Wiley-Interscience, New York (1979) (393 pp.)

Tsang, O., Kirk, J.G.: The inverse Compton catastrophe and high brightness temperature radio sources. Astron. Astrophys. **463**, 145–152 (2007). doi:10.1051/0004-6361:20066502

Wagner, S.J., Witzel, A.: Intraday variability in quasars and BL Lac objects. Annu. Rev. Astron. Astrophys. **33**, 163–198 (1995). doi:10.1146/annurev.aa.33.090195.001115